Evidence for Perceptual "Trapping" and Adaptation in Multistable Binocular Rivalry

Satoru Suzuki[1] and Marcia Grabowecky
Northwestern University
Department of Psychology
2029 Sheridan Road
Evanston, Illinois 60208

Summary

When a different pattern is presented to each eye, the perceived image spontaneously alternates between the two patterns (binocular rivalry); the dynamics of these bistable alternations are known to be stochastic. Examining multistable binocular rivalry (involving four dominant percepts), we demonstrated *path dependence* and *on-line adaptation*, which were equivalent whether perceived patterns were formed by single-eye dominance or by mixed-eye dominance. The spontaneous perceptual transitions tended to get *trapped* within a pair of related global patterns (e.g., opponent shapes and symmetric patterns), and during such *trapping*, the probability of returning to the repeatedly experienced patterns gradually decreased (postselection pattern adaptation). These results suggest that the structure of global shape coding and its adaptation play a critical role in directing spontaneous alternations of visual awareness in perceptual multistability.

Introduction

Perceptual bistability is a well-known phenomenon (e.g., Attneave, 1971). Typical examples include the Necker cube (spontaneous alternation of two depth organizations), Rubin's face-vase (alternation of two figure-ground organizations, either two faces or a vase), bistable apparent motion (alternation of two directions of motion), and binocular rivalry (alternation of two dissimilar images, one presented to each eye). In all cases, while the stimulus remains constant, conscious experience spontaneously alternates between two mutually exclusive percepts. An observer's intention (attempt to bias a particular percept) may increase the relative dominance of the desired percept to a limited degree (e.g., Lack, 1974, 1978; Ramachandran and Anstis, 1983; Peterson and Gibson, 1991; Peterson et al., 1991; Cavanagh, 1992; Suzuki and Peterson, 2000; Verstraten et al., 2000; Ming and Tong, 2002, VSS, abstract). However, the process underlying bistable rivalry is believed to be stochastic because the length of a particular dominance phase cannot be predicted on the basis of the preceding dynamics of dominance alternations. This has been indicated by the lack of autocorrelation, Lathrop values (Lathrop, 1966) not significantly different from unity (e.g., Fox and Herrmann, 1967; Blake et al., 1971; Borsellino et al., 1972; Taylor and Aldridge, 1974; Wade, 1975; Lehky, 1988; Logothetis et al., 1996), and the lack of evidence of deterministic chaos at least for binocular

rivalry (e.g., Richards et al., 1994; Lehky, 1995). Models of bistable rivalry (binocular rivalry in particular) postulate that perceptual alternations are due to adaptive nonlinear inhibitory interactions between channels that respond to the two competing percepts, with random neural noise (either in the rivaling inputs or in the inhibitory interactions) generating the stochastic properties (e.g., Sugie, 1982; Lehky, 1988; Blake, 1989).

Though the dynamics of bistable rivalry (alternations between two competing percepts) has been studied extensively, relatively little is known about the dynamics of multistable rivalry (i.e., alternations among multiple competing percepts, Diaz-Caneja, 1928; Cogan, 1972; Kovács et al., 1996). Importantly, unlike bistable rivalry in which only temporal parameters (e.g., dominance-phase durations) are informative, in multistable rivalry, differential transition probabilities may also provide insights into the dynamics of perceptual multistability.

Suppose that a given stimulus generates four competing (perceived) images, *A*, *B*, *C*, and *D*. Any systematic asymmetry in transition probabilities could reveal potential dynamical structure in multistable rivalry. For example, if a transition to *A* is more probable following *B* than following *C* or *D*, this would indicate a *path dependence* (i.e., getting to *A* is more likely from *B* than from *C* or *D*). Furthermore, the course of multistable rivalry might also be affected by pattern adaptation such that transition probabilities to return to recently experienced images might be reduced. For example, probabilities of switching to *A* might be smaller following a sequence of …*ABAB* than following a sequence of …*CDCD*. Such a result would provide evidence of pattern adaptation occurring after rivalry is resolved and a percept is selected because the component parts of all possible multistable percepts are present in the stimulus and thus are activated in neural representations prior to selection. To our knowledge, adaptation to spontaneously perceived patterns during perceptual multistability has not been previously demonstrated.

To study the dynamics of multistable rivalry, it was critical to design stimuli which generated multiple competing percepts which were all stable and clearly identifiable. Furthermore, we reasoned that *related* images whose neural representations are presumably strongly connected (e.g., images processed by neighboring feature columns in IT; e.g., Fujita et al., 1992; Tanaka, 1996; Wang et al., 2000; Tsunoda et al., 2001) might produce path dependence such that perceptual transitions might be more frequent between related images than between unrelated images. While it is difficult to define relatedness, we drew on prior findings that opponent shape aftereffects occurred for some basic shape attributes, including aspect ratio, taper, curvature, skew, and convexity (e.g., Regan and Hamstra, 1992; Suzuki and Cavanagh, 1998; Suzuki, 2001; Suzuki, 2002, VSS, abstract). Shapes that produce opposite aftereffects (e.g., convex and concave shapes) may be considered related because they are likely to be involved in opponent coding of the same shape attribute (e.g., convexity). Thus, the two primary stimulus sets we used, the *hourglass-dia-*

[1]Correspondence: satoru@northwestern.edu

mond-chevron stimulus set and the *triangle-parallelogram stimulus set*, were designed to generate pairs of rivaling opponent shapes. If perceptual transitions were more prevalent between related shapes, they might be more prevalent between opponent shapes than between non-opponent shapes. We also used two additional control stimulus sets that did not generate opponent shapes. These differing stimulus sets allowed us to contrast two potential mechanisms of path dependence, one based on feedback from global shape coding and the other based on low-level ocular interactions.

These four sets of stimuli, the two primary sets with opponent shapes and the two control sets without opponent shapes, were each presented dichoptically (one shape to each eye) using a stereoscope. The hourglass-diamond-chevron stimulus set was shown either as a pair of an hourglass and a diamond (Figure 1A), or a pair of a left-pointing and a right-pointing chevron (Figure 1B). In either case, when seen through the stereoscope, the overall contour pattern was identical and the perceived image was *multistable*, alternating among four clear shapes, (1) hourglass, (2) diamond, (3) left-pointing chevron, and (4) right-pointing chevron. The hourglass and the diamond had opponent convexity, and the two chevrons had opponent curvature. Note that two of the four perceived shapes resulted from complete dominance of a single eye, *single-eye dominance*, whereas the remaining two shapes resulted from each eye dominating one side of the image, *mixed-eye dominance (or pattern dominance)*. For example, when the hourglass was presented to the left eye and the diamond was presented to the right eye (Figure 1A), perceptual dominance of the hourglass and the diamond corresponded to complete dominance of the left-eye image and the right-eye image, respectively. In contrast, perceptual dominance of the right-pointing chevron corresponded to the left-eye image being dominant on the left side while the right-eye image was dominant on the right side; perceptual dominance of the left-pointing chevron corresponded to the left-eye image being dominant on the right side while the right-eye image was dominant on the left side.

Similarly, the triangle-parallelogram stimulus set was shown either as a pair of an upright and an inverted triangle (Figure 1C), or a pair of a left-skewed and a right-skewed parallelogram (Figure 1D). Again, when seen through the stereoscope, the overall contour pattern was identical in either case and the perceived image was multistable, alternating among (1) upright triangle, (2) inverted triangle, (3) left-skewed parallelogram, and (4) right-skewed parallelogram. This stimulus set also generated opponent pairs of rivaling images in that the two triangles had opponent taper (upward versus downward), and the two parallelograms had opponent skew (left versus right).

The control stimulus sets were also multistable with four dominant percepts as shown in Figures 1E and 1F (the *circle-line-90° U stimulus set*) and Figures 1G and 1H (the *separate-shape stimulus set*), but the perceived images for these control stimuli did not include opponent pairs of shapes.

To summarize, we hypothesized that the dynamics of multistable perceptual rivalry might show evidence of structure in the form of path dependence. Specifically,

we hypothesized that perceptual transitions might be more frequent between related images (as defined by opponent shape aftereffects) than between unrelated images. We also expected that the visual system might adapt to spontaneously perceived images during multistable rivalry, resulting in reduced transition probabilities to return to recently experienced images.

Results

We first analyzed dominance-phase durations to confirm multistability of our stimuli. We then analyzed transition probabilities to provide evidence for (1) path dependence and (2) postselection adaptation during multistable rivalry.

Dominance-Duration Analysis and Confirmation of Multistability

To confirm that our stimulus sets were multistable, we examined dominance-phase durations (Figure 2). For each stimulus set, the overall % dominance

$$\left(\frac{\text{Total time of dominance for image X}}{\text{Total time of observation}} \times 100\% \right)$$

and the average duration per dominance phase are shown for each perceived image under "IMAGE EFFECT" in Figure 2. Patterns with bilateral symmetry tended to dominate longer than those without bilateral symmetry (Figures 2A–2C); the concentric texture was particularly dominant (Figure 2C). Overall, however, each stimulus set was multistable in that all four images dominated for substantial percentages of time. Under "EYE EFFECT" in Figure 2, the % dominance and the average duration per dominance phase are presented separately for single-eye dominance and mixed-eye dominance. The fact that perceived images resulted from mixed-eye dominance for substantial percentages of time again confirms that the stimulus sets used were multistable. Furthermore, the average duration per dominance phase (1.5–2.7 s) was comparable to those previously reported in binocular rivalry, and was longer for single-eye dominance than for mixed-eye dominance (consistent with Kovács et al., 1996). Distributions of the normalized dominance duration are also shown (the data for each perceived image from each observer for each type of eye dominance were trimmed using 3*SD* criterion and divided by the mean before they were combined). Following the convention (e.g., Levelt, 1965; Fox and Herrmann, 1967; Blake et al., 1971; Wade, 1974, 1975; Kovács et al., 1996), and to allow comparison between our data and those obtained by others, these distributions were fit by γ functions,

$$f(x) = \frac{\lambda^r}{(r-1)!} x^{r-1} e^{-\lambda x},$$

where $r = \lambda$ because the means have been normalized to 1. The range of r values obtained were comparable to those reported previously; r's were larger for mixed-eye dominance than for single-eye dominance (consistent with Kovács et al., 1996). The fits appear to be poor for the hourglass-diamond-chevron stimulus set and for the triangle-parallelogram stimulus set, particularly for
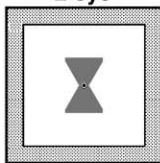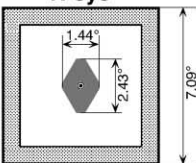
Multistable (quadra-stable) stimulus sets

Figure 1. An Illustration of the Four Multistable Stimulus Sets Used

The hourglass-diamond-chevron stimulus set (A and B) and the triangle-parallelogram stimulus set (C and D) were used in the main experiment. The circle-line-90° U stimulus set (E and F) and the separate-shape stimulus set (G and H) were used in the control experiments. The assignment of the patterns to the two eyes was counterbalanced. When viewed through the stereoscope, each stimulus yielded four clearly dominant percepts. Two of those percepts were consistent with an exclusive dominance of either eye, labeled as "Single-eye dominance." The other two percepts were consistent with each eye dominating on one side of the image, labeled as "Mixed-eye dominance" (see A and B for an illustration); various other possible combinations of complementary images did not occur in mixed-eye dominance presumably because the actually observed forms were supported by image grouping factors such as eye of origin, contour continuity, and symmetry. Numbers on the illustrations refer to degrees of visual angle of the actual stimuli. Note that attempting to free-fuse these images may produce fused 3D depth organizations instead of multistable rivalry; this did not occur with the actual stimuli. Some initial familiarization time may be required to start seeing clear multistable rivalry using these illustrations.

	IMAGE EFFECT				EYE EFFECT		Dominance duration distribution (set to common base)	
					Single-eye dominance	Mixed-eye dominance	Single-eye dominance	Mixed-eye dominance
A Hourglass-diamond-chevron stimulus set							N=3373 $\lambda=r=3.79$	N=2421 $\lambda=r=4.35$
% dominance M	37	27	16	20	57	43		
(SE)	(2)	(2)	(2)	(1)	(2)	(2)		
Duration per dominance (sec.) M	1.80	1.54	1.57	1.65	1.69	1.61		
(SE)	(0.29)	(0.29)	(0.25)	(0.25)	(0.29)	(0.25)		
B Triangle-parallelogram stimulus set							N=3778 $\lambda=r=3.10$	N=1596 $\lambda=r=4.67$
% dominance M	27	27	22	24	68	32		
(SE)	(3)	(2)	(3)	(2)	(4)	(4)		
Duration per dominance (sec.) M	1.97	2.01	1.71	1.79	2.02	1.74		
(SE)	(0.51)	(0.51)	(0.29)	(0.40)	(0.51)	(0.35)		
C Circle-line-90° U stimulus set							N=2293 $\lambda=r=3.71$	N=1801 $\lambda=r=4.33$
% dominance M	50	21	16	13	60	40		
(SE)	(5)	(3)	(1)	(2)	(2)	(2)		
Duration per dominance (sec.) M	2.68	1.72	1.69	1.77	2.24	1.80		
(SE)	(0.41)	(0.19)	(0.16)	(0.19)	(0.25)	(0.19)		
D Separate-shape stimulus set							N=1737 $\lambda=r=3.52$	N=2065 $\lambda=r=5.52$
% dominance M	27	20	27	26	47	53		
(SE)	(1)	(1)	(2)	(2)	(3)	(3)		
Duration per dominance (sec.) M	2.21	2.04	2.36	2.35	2.44	2.06		
(SE)	(0.14)	(0.18)	(0.37)	(0.31)	(0.40)	(0.10)		

Figure 2. Dominance-Phase Durations Are Shown as the Overall % of Time in a Dominance Phase and as the Average Duration per Dominance Phase

For each of the four stimulus sets, the dominance durations are shown for individual perceived images (under IMAGE EFFECT) as well as for the two types of eye dominance, single-eye dominance and mixed-eye dominance (under EYE EFFECT). The image effect and the eye effect were additive (no evidence of interaction) for all stimulus sets. The SEM's (in parentheses) were computed using observers as the random effect. The distributions of dominance-phase durations (after normalizing to a common base) are also shown separately for the two types of eye dominance. The continuous functions represent γ function fits; the λ and r (equal due to normalization) were obtained from the fits.

single-eye dominance. However, the appropriateness of γ functions (rather than other functions such as Lognormal and Weibull) for fitting distributions of dominance durations in binocular rivalry has been disputed (e.g., Cogan, 1973). For the purpose of the current study, we conclude that our baseline data for dominance-phase durations (1) clearly indicated perceptual multistability and (2) were generally consistent with those previously reported in binocular rivalry.

Transition-Probability Analysis
Evidence for Path Dependence—Perceptual Trapping
When the hourglass-diamond-chevron stimulus set was viewed, regardless of which pair was presented (the hourglass-diamond pair, Figure 1A, or the chevron pair, Figure 1B), the perceived shape alternated between the hourglass and the diamond and between the right and the left chevron substantially more frequently than expected by chance. Similarly, when the triangle-parallelogram stimulus set was viewed, regardless of which pair was presented (the triangle pair, Figure 1C, or the parallelogram pair, Figure 1D), the perceived shape alternated between the upright and the inverted triangle and between the right and the left parallelogram more fre-

quently than expected by chance. We call this phenomenon *perceptual trapping* because percepts tended to get trapped within specific pairs of shapes.

These observations were confirmed by analyzing conditional (transition) probabilities, *p(current percept| preceding percept)*. If there was no trapping, the probability of seeing each dominant shape should be independent of which shape was seen just prior to it. For the hourglass-diamond-chevron stimulus set, for example, the probability of making a perceptual transition to the hourglass should be the same regardless of whether the currently perceived shape was the diamond, the left chevron, or the right chevron. In other words, the three transition probabilities, *p(hourglass|diamond)*, *p(hourglass|left chevron)*, and *p(hourglass|right chevron)* should have been equal if there was no path dependence. More conveniently (for data plotting purposes), the *relative transition probability*, p_r, can be defined as,

$$p_r(A|B) = \frac{p(A|B)}{p(A|B) + p(A|C) + p(A|D)} \quad (1)$$

which should be 1/3 for all transition probabilities if there was no path dependence. If instead there was trapping between the hourglass and the diamond, p_r(hourglass|
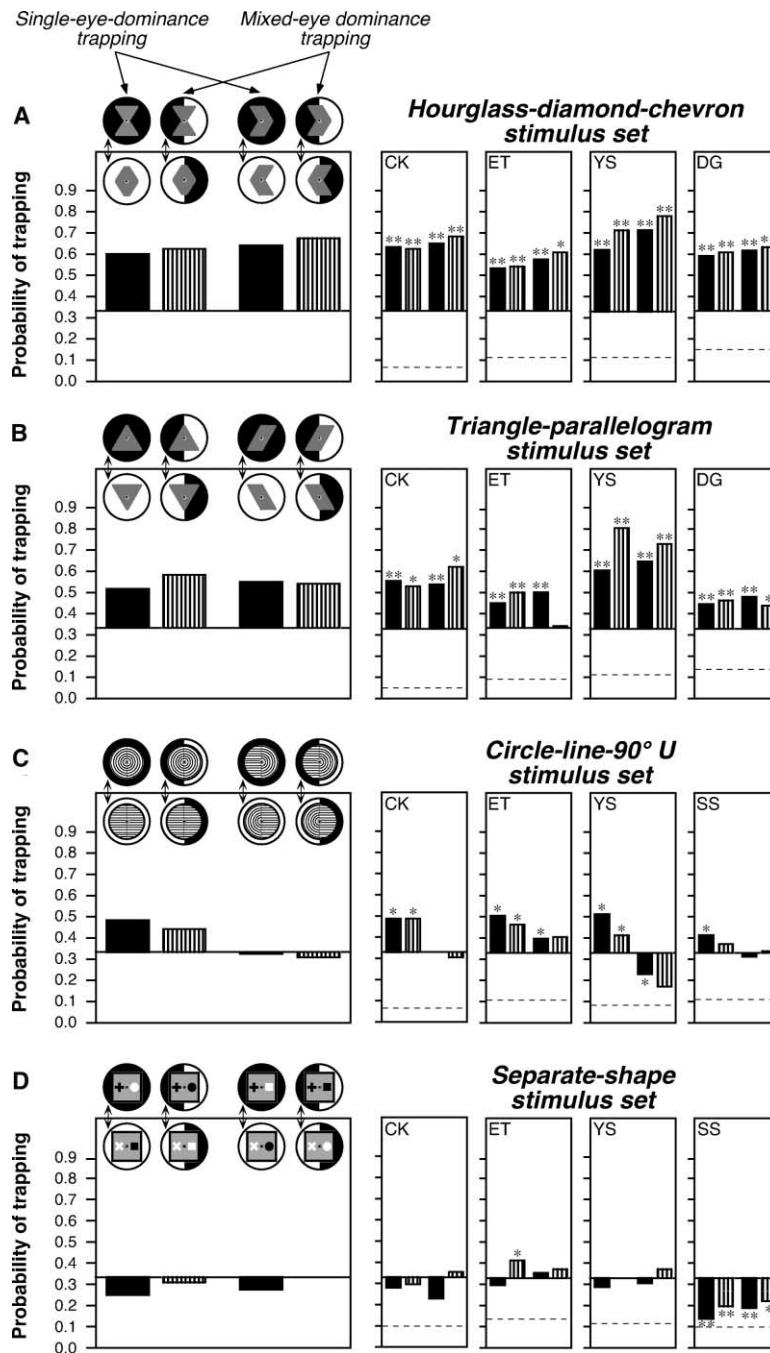
Figure 3. The Probability of First-Order Trapping

The probability of trapping (see Equation 1) is shown for the main experiment (A and B) and for the control experiments (C and D). Data are plotted separately for "Single-eye-dominance trapping" in which the trapping images were both consistent with single-eye dominance (black bars) and for "Mixed-eye-dominance trapping" in which the trapping images were both consistent with mixed-eye dominance (striped bars). The average data are shown in the left panels with corresponding percept icons; the black and white backgrounds shown behind the percept icons represent the pattern of eye dominance (the same eye being dominant in the same colored region). The right panels show data from individual observers. The chance level of 1/3 is based on the assumption that each dominant image was processed as a unit (see text). The asterisks indicate statistically significant (p < 0.05) deviations from chance based on χ^2 tests; the single asterisks indicate that trapping significantly deviated from chance for only one of the two directions of transition (e.g., significant from left to right parallelogram but not significant from right to left parallelogram); the double asterisks indicate that trapping was significant for both directions. The dashed lines indicate estimates of chance probabilities of trapping based on the assumption that binocular rivalry occurred independently on the left and right sides (see Experimental Procedures).

diamond) and p_r(diamond|hourglass) should have been greater than 1/3, and if there was trapping between the two chevrons, p_r(left chevron|right chevron) and p_r(right chevron|left chevron) should have been greater than 1/3; we thus refer to these relative transition probabilities as "*probabilities of trapping*" with chance being 1/3. The same logic holds for the triangle-parallelogram stimulus set. Note that the trapping effects examined here were first-order effects because path dependencies were evaluated with respect to only the immediately preceding percept. We also assumed that the visual system processed each of the four rivaling images as a unit. As discussed later, if the four images occurred as a result

of independent local rivalry, the expected chance probability of trapping would be even less.

The deviation of each transition probability from the null hypothesis (no path dependence) was evaluated for each observer using χ^2 tests (using p < 0.05 criterion). In Figure 3, the relative transition probabilities for each trapping pair (e.g., the hourglass and the diamond) have been averaged for the two directions (e.g., p_r[hourglass|diamond] and p_r[diamond|hourglass]). A double asterisk indicates that the deviation from chance was significant for both directions; a single asterisk indicates that the deviation was statistically significant only for one direction (but the trend for the other direction was always

consistent for both the hourglass-diamond-chevron stimulus set and for the triangle-parallelogram stimulus set). The means across observers are shown in the left panels along with the percept icons (the black and white backgrounds in the percept icons represent dominance of different eyes). Note that each case of trapping was consistent with either alternations between single-eye-dominant images or alternations between mixed-eye-dominant images. As discussed below, the fact that trapping occurred between images with complementary patterns of eye dominance raised the possibility that spatially synchronized changes in eye dominance might contribute to trapping.

As is evident in Figures 3A and 3B, the results confirmed perceptual trapping; the hourglass-diamond transitions, the left-chevron-right-chevron transitions, the up-triangle-down-triangle transitions, and the left-parallelogram-right-parallelogram transitions all occurred substantially above chance (1/3) whether the images were seen due to single-eye dominance (black bars) or mixed-eye dominance (striped bars). Transitions between all other pairs of images (e.g., diamond and right-chevron, down-triangle and left-parallelogram, etc.) were not elevated. The data were consistent across observers as shown in the right panels; the only exception was that the left-parallelogram-right-parallelogram trapping in the mixed-eye case was not statistically different from chance for observer E.T. The results thus appear to be consistent with our initial hypothesis that perceptual transitions in multistable rivalry might be more likely between related opponent shapes (which are presumably involved in coding of a common shape attribute).

As indicated above, however, all cases of trapping occurred as alternations between images with complementary patterns of eye dominance. Thus, trapping could be explained if changes in eye dominance tended to be synchronized across the visual field—the *change-synchronization hypothesis*. Specifically, all cases of trapping shown in Figures 3A and 3B could be explained if eye dominance on the right side and the left side tended to change together. The key prediction of this general change-synchronization hypothesis was that similar trapping should occur in *any* multistable binocular rivalry regardless of the figural relationships among the rivaling patterns. To contrast this general, pattern-independent prediction of trapping based on the change-synchronization hypothesis with the opponent-shape hypothesis, we tested control stimuli that did not generate image pairs that produced opponent aftereffects.

The circle-line-90° U stimulus set (adapted from Diaz-Caneja, 1928) consisted of texture patterns rather than shapes; the perceived pattern alternated among (1) concentric circles, (2) horizontal lines, (3) a 90° clockwise-rotated U texture, and (4) a 90° counterclockwise-rotated U texture (see Figures 1E and 1F). In the separate-shape stimulus set, the left and the right sides were spatially separated so that each dominant image consisted of a configuration of two shapes rather than a single unified shape; the perceived configuration alternated among (1) a "+" on the left and a circle on the right, (2) an "x" on the left and a square on the right, (3) a "+" on the left and a square on the right, and (4) an "x" on the left and a circle on the right (see Figures 1G

and 1H). The contrast polarity was reversed in the two eyes to induce clear rivalry. The change-synchronization hypothesis predicted that trapping should occur both within a pair of single-eye-dominant images and within a pair of mixed-eye-dominant images for these control stimulus sets, just as for the hourglass-diamond-chevron and the triangle-parallelogram stimulus sets that generated opponent shape pairs.

As shown in Figures 3C and 3D, the overall results did not support the change-synchronization hypothesis. For the circle-line-90° U stimulus set, although some trapping occurred between the circles and the lines (left bars in Figure 3C), trapping was nearly absent for the two 90° U patterns (right bars in Figure 3C), regardless of whether the dominance was single-eye or mixed-eye. For the separate-shape stimulus set, virtually no trapping occurred (Figure 3D). Interestingly, for observer S.S., the trapping was consistently *below* 1/3. This, however, does not imply that trapping was actively inhibited.

As mentioned earlier, in estimating the chance occurrence of trapping to be 1/3, *we assumed that the visual system processed each of the four rivaling images as a unit*. However, if the left and the right sides were processed separately, binocular rivalry could occur relatively independently on either side. Then, the kind of trapping obtained with the hourglass-diamond-chevron stimulus set and the triangle-parallelogram stimulus set, which required synchronous changes in eye dominance on both sides, would have been even less likely than 1/3 by chance. The dashed lines in Figure 3 indicate conservative (upper-end) estimates of the chance probabilities of trapping (synchronous changes on both sides) on the assumption of independent rivalry on either side (see the Experimental Procedures section for the computation of these estimates).

The fact that the actual occurrences of trapping tended to be closer to 1/3 rather than to the dashed lines (except for SS) even for the separate-shape stimulus set indicates that even when the two sides did not generate a single global shape, changes in eye dominance tended to be synchronized for the two sides *to the extent that each perceived two-shape configuration was processed as a unit, that is, to the extent that asynchronous transitions (e.g., from hourglass to left chevron or to right chevron) were only twice as likely as synchronous transitions (e.g., from hourglass to diamond)*. It is thus possible that a change-synchronizing binocular interaction might account for the fact that trapping tended not to dip below 1/3. However, it does not explain why trapping was particularly strong for opponent shapes, that is, between the hourglass and the diamond, between the left-pointing chevron and the right-pointing chevron, between the up triangle and the down triangle, and between the left-skewed parallelogram and the right-skewed parallelogram (Figures 3A and 3B). Elevated trapping was also present but less robust for bilaterally symmetric textures, that is, between the concentric circles and the horizontal lines (Figure 3C, left bars). The fact that trapping beyond 1/3 was not obtained for the 90° U patterns indicates that having the two sides form a coherent shape per se does not guarantee trapping beyond unitized processing of each perceived image (Figure 3C, right bars). Finally, though trapping beyond 1/3 did not occur for the separate-shape stimulus set,

there was a small, but consistent, tendency for trapping to be slightly greater when the left and the right shapes had the same contrast polarity (both black or both white; Figure 3D, striped bars) than when they had different contrast polarities (Figure 3D, solid bars). We next evaluated whether the visual system adapted to the perceived images during trapping.

Evidence for Postselection Adaptation during Trapping

We examined whether there was evidence of adaptation to perceived images during a trapping sequence in which a given image was perceived repeatedly in temporal proximity. For example, for the hourglass-diamond-chevron stimulus set, there were four types of trapping sequences, …(*notD*)*HDHD*.., …(*notH*)*DHDH*.., …(*notR*)*LRLR*.., and …(*notL*)*RLRL*.., where *H*, *D*, *L*, and *R* indicate perception of the hourglass, the diamond, the left chevron, and the right chevron, respectively. For each type of sequence, we examined whether the transition probabilities for continued trapping, $p(H|D)$, $p(D|H)$, $p(L|R)$, and $p(R|L)$, diminished within the relevant trapping sequence as dominance of the same image continued to occur. Note that longer trapping sequences would be generally decreasingly frequent even if there was no adaptation, that is, even if the transition probabilities were stationary (i.e., constant in the course of a trapping sequence). In order to show evidence of adaptation, sequential reductions in *transition probabilities* must be demonstrated.

For example, within a "…(*notH*)*DH*…" trapping sequence, the probability of a *[D→H]* transition, $p(H|D)$, was computed following 0 prior occurrences of *H* (i.e., "…(*notH*)*[D→H]*…"), following 1 prior occurrence of *H* (i.e., "…(*notH*)*DH[D→H]*…"), following 2 prior occurrences of *H* (i.e., "…(*notH*)*DHDH[D→H]*…"), and so on, until the number of incidences of the relevant cases (i.e., the denominator frequency of the transition probability) dropped to less than 10. To be consistent with the trapping analyses shown above, the transition probabilities were normalized (e.g.,

$$p_r(H|D) = \frac{p(H|D)}{p(H|D) + p(H|L) + p(H|R)};$$

see Equation 1) such that chance (assuming each perceived image was processed as a unit) would be 1/3.

A systematic decrease in the *[D→H]* transition probability following 0, 1, 2…, prior percepts of *H* during a "…(*notH*)*DHDH*…" trapping sequence would indicate adaptation to the perception of *H* during the course of trapping. Evidence of adaptation to *H* can thus be indexed as the negative linear slope of the *[D→H]* transition probability as a function of the number of prior percepts of *H* during a trapping sequence—an *adaptation slope*. This within-trapping adaptation slope was computed for each of the four perceived shapes (e.g., *H*, *D*, *R*, and *L* for the hourglass-diamond-chevron stimulus set), separately for the single-eye dominance trapping and the mixed-eye-dominance trapping. Each observer thus yielded eight adaptation slopes for each stimulus set (except where there were too few [<10] trapping sequences of sufficient length to compute the *A→B* transition probability following at least 1 prior percept of *B*). Frequency distributions of the adaptation slope

are shown in the right panels in Figure 4 (the striped bars for the mixed-eye-dominance trapping are stacked on the solid bars for the single-eye dominance trapping).

For the hourglass-diamond-chevron and the triangle-parallelogram stimulus sets (Figures 4A and 4B), the slope distributions were clearly shifted in the negative direction, indicating adaptation. T tests using individual cases as the random effect confirmed this negative shift ($p < 0.05$, 2-tailed) for both stimulus sets and for both single-eye dominance trapping and mixed-eye-dominance trapping.

There was no evidence of adaptation for the circle-line-90° U stimulus set; the slope distribution was centered around zero (Figure 4C; nonsignificant t values for either type of eye dominance). For the separate-shape stimulus set, the slope distribution was also centered around zero (Figure 4D), showing little evidence of adaptation. Note, however, that the distribution for mixed-eye-dominance trapping (striped bars) was slightly negatively shifted ($p < 0.08$). This suggests that some process of color- and/or contrast-polarity-based grouping might show weak adaptation because the left and right shapes were both black or both white for mixed-eye-dominance trapping for these stimuli (see the upper row of percept icons in Figure 4D).

The overall adaptation trends are also shown in the left panel in Figure 4; the overall probability of continued *A→B* trapping, $p_r(B|A)$, is shown as a function of the number of prior percepts of *B* within a trapping sequence for each stimulus set (averaged across the four observers and the four perceived images, but averaged separately for the single-eye dominance trapping and the mixed-eye-dominance trapping). Because the length of the trapping sequences varied across the observers and the perceived images, the means are shown for the cases where at least three of the four observers contributed data for at least one of the four perceived images; the empty cells were filled using the last available values; for example, if *A→B* transition probabilities were unavailable from an observer beyond a single incidence of prior *B*, that value was substituted for the transition probabilities following two and greater incidences of prior *B*. Due to these averaging procedures, these overall adaptation functions underestimate the actual degree of adaptation and are useful primarily to help visualize the adaptation trends.

Nevertheless, it is noteworthy from these overall adaptation functions that the hourglass-diamond-chevron and the triangle-parallelogram stimulus sets which yielded reliably negative adaptation slopes also produced strong trapping. One might thus postulate that stronger trapping generally might be conducive to greater adaptation (e.g., a floor effect). If so, stronger trapping should be associated with greater negative adaptation slopes also within each stimulus set. We thus examined, for each stimulus set, the correlation between the distribution of adaptation slopes shown in the right panel in Figure 4 and the corresponding first-order trapping (computed using Equation 1). The outliers were removed based on Bivariate Normal Ellipse at p = 0.99 (*SAS* statistics package); no more than 1 point was removed from the analysis for each stimulus set. If stronger trapping generally yielded greater adaptation
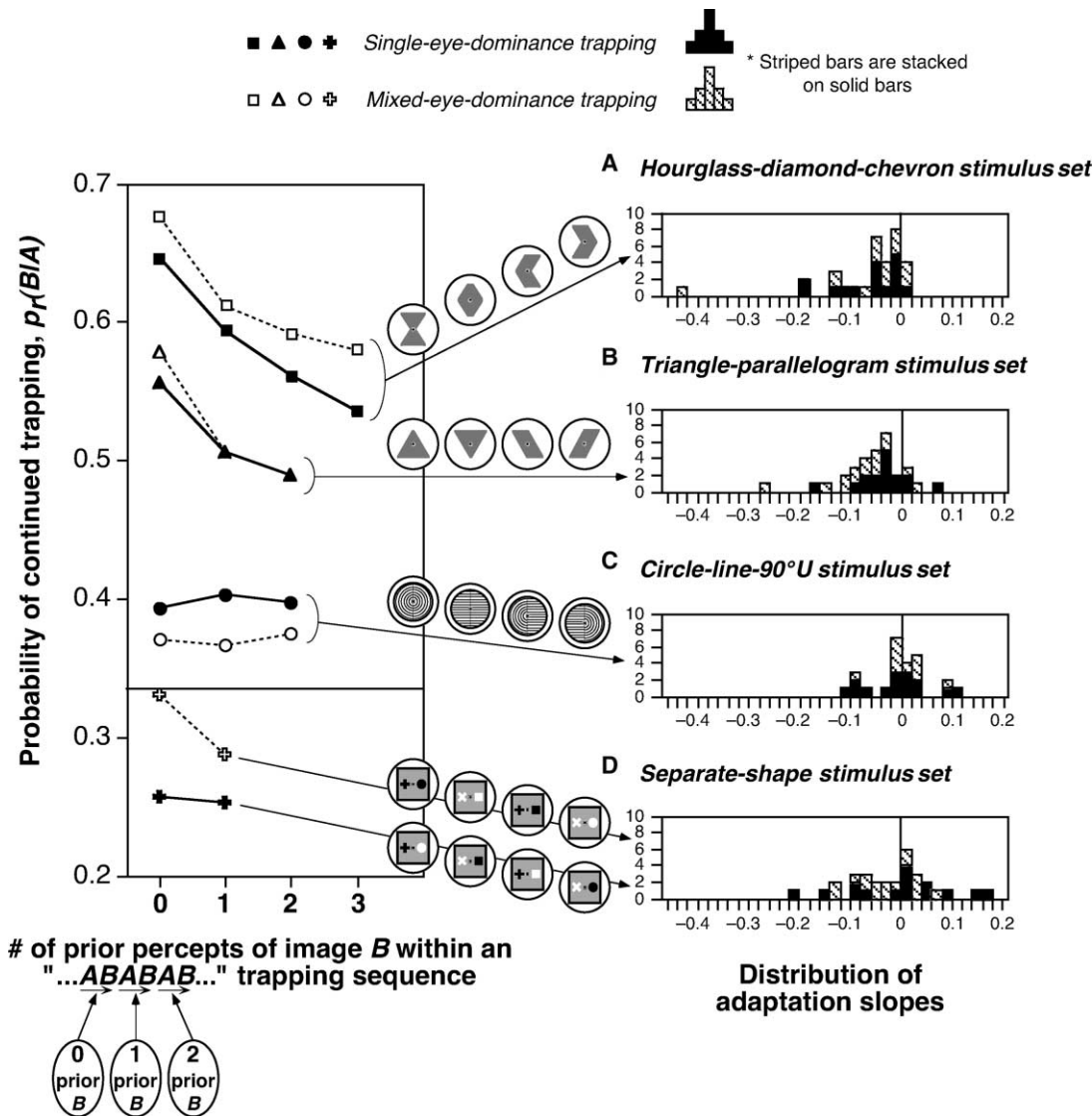
Figure 4. Changes in Transition Probability during Trapping

In the left panel, the relative probability of continued trapping, $p_r(B|A)$, is plotted as a function of the number of prior incidences of the dominance of B within a trapping sequence of "...ABAB..." To illustrate overall trends, the data were averaged for each stimulus set across observers and across all perceived images, but averaged separately for the single-eye-dominance trapping (filled symbols) and the mixed-eye-dominance trapping (open symbols). The linear slope of the functions illustrated in the left panel was computed for each relevant transition probability (representing adaptation to each perceived image during trapping under each of the two types of eye dominance) for each observer, and the distributions of these *adaptation slopes* are plotted in the right panels. Negative values indicate adaptation (sequential decreases in transition probabilities to return to repeatedly perceived images) during trapping. Note that for the separate-shape stimulus set (D), the left and the right shapes had the same color during mixed-eye dominance, but different colors during single-eye dominance (illustrated with separate rows of percept icons; also see Figure 3D). For the rest of the stimulus sets, the perceived images were identical during the two types of eye dominance.

(larger negative slopes), the correlation should be negative for each stimulus set.

None of the correlations (all positive and varying in r^2 from 0.01 to 0.07) was significantly different from zero (p < 0.05, 2-tailed). This lack of negative correlation was substantial considering the fact that the strength of first-order trapping varied widely from one trapping pair to another and from observer to observer for each stimulus set (about 0.5–0.8 for the hourglass-diamond-chevron stimulus set, about 0.4–0.8 for the triangle-parallelogram stimulus set, about 0.3–0.7 for the circle-line-90° U stim-

ulus set, and about 0.2–0.4 for the separate-shape stimulus set). Notably, as shown in Figure 3C, the circle-line pair, but not the left-right-U pair, yielded significant trapping for the circle-line-90° U stimulus set, but the lack of correlation indicated that there was no trend for the adaptation slopes to be more negative for the circle-line pair. Thus, these analyses suggest that stronger trapping per se (or a potential floor effect) does not account for the reliably negative adaptation slopes obtained specifically for the hourglass-diamond-chevron and the triangle-parallelogram stimulus sets.

So far, we have reported that adaptation occurred during trapping for the hourglass-diamond-chevron and the triangle-parallelogram stimulus sets in terms of sequential reductions in the transition probability to return to repeatedly experienced images. We next analyzed whether adaptation also occurred in terms of sequential reductions in dominance-phase duration during trapping, as might be predicted from desensitization of neural units responding to perceived images.

Dominance-phase durations for each perceived image (e.g., *H*) were averaged for its 1st occurrence, 2nd occurrence, 3rd occurrence, and so on, within a trapping sequence; the series was terminated when fewer than five durations were available to compute the average. As before, this adaptation series was computed for each trapping image for each observer, separately for the single-eye dominance trapping and the mixed-eye-dominance trapping. The linear slope was then computed for each series (except where the trapping was infrequent and the 2nd incidence of a given image within a trapping sequence occurred fewer than five times). To normalize for variations in average dominance-phase durations across images and observers, slopes were computed as proportional changes in dominance duration relative to the corresponding series means (e.g., slope = −0.1 would indicate that the dominance duration decreased by 10% of the mean per each repetition of the same image during trapping). The distribution of the slopes is shown for each stimulus set in the right panels in Figure 5 (again, the striped bars for the mixed-eye-dominance trapping are stacked on the solid bars for the single-eye dominance trapping).

Clearly, there was no evidence of adaptation (i.e., no negative shifts for any of the distributions). In fact, the slope distributions were positively shifted for the hourglass-diamond-chevron and the triangle-parallelogram stimulus sets (Figures 5A and 5B); t tests using individual cases as the random effect confirmed that these positive shifts were significant ($p < 0.05$, 2-tailed) except for the mixed-eye-dominance trapping for the triangle-parallelogram stimulus set due to the two outliers in the far negative range (Figure 5B). For the circle-line-90° U and the separate-shape stimulus sets, the slope distributions were centered around zero (nonsignificant t values).

The overall trends are shown in the left panel in Figure 5; for each stimulus set, the average dominance-phase duration (normalized relative to 1st dominance) is plotted for the kth dominance of the same image within a trapping sequence. The data have been averaged across the four observers and the four perceived images (but averaged separately for the single-eye-dominance trapping and the mixed-eye-dominance trapping). Because the length of the trapping sequences varied across the perceived images and the observers, the means are shown for the cases where each observer contributed data for at least one of the four perceived images; the empty cells were filled using the last available values as before. It is clear that no adaptation (decreasing) trend is evident for dominance-phase duration.

To summarize the adaptation analyses, for the hourglass-diamond-chevron and the triangle-parallelogram stimulus sets, reliable adaptation occurred for transition probability during the course of trapping in that the prob-

ability to return to a recently experienced image diminished with repetition. Similar adaptation, however, did not occur for dominance-phase duration. Interestingly, dominance-phase duration tended to slightly increase over the course of trapping as if perception of the trapping images became increasingly more stable over the course of a trapping sequence. No evidence of adaptation during trapping was obtained for the two control stimuli either for transition probability or for dominance-phase duration.

Discussion

Using a multistable binocular rivalry paradigm, we have demonstrated path dependence and postselection adaptation in perceptual multistability. First, spontaneous perceptual transitions tended to get trapped within related pairs of shapes. Second, the probability of continued trapping tended to decrease over the course of a trapping sequence for opponent pairs of shapes, indicating that the visual system can adapt to a pair of repeatedly experienced images during multistable rivalry.

Because trapping manifested as alternations between image pairs consisting of complementary patterns of eye dominance (Figure 3), a general, stimulus feature-independent tendency for eye dominance to change synchronously across the visual field might have contributed. Such general change synchronization might account for the fact that for all stimulus sets we used (the opponent sets as well as the control sets), trapping rarely fell below 1/3 (a chance level given unitized processing of each dominant image), and it always remained above the level expected from independent rivalry on the left and right sides (Figure 3, dashed lines). In other words, a general tendency for eye dominance to change synchronously across the visual field might affect multistable binocular rivalry to the extent that each stable perceived image tended to compete as a unit.

This general change-synchronization hypothesis, however, could not account for the fact that strong trapping (well beyond 1/3) occurred for only certain pairs of perceived images. The fact that trapping did not occur for arbitrary pairs of rivaling images is corroborated by a previous study by Cogan (1972) that showed no evidence of trapping using line segments as the rivaling stimuli. She examined binocular rivalry between a vertical line (presented to one eye) and an overlapping horizontal line (presented to the other eye), and obtained multistability due to single-eye dominance (seeing either the vertical line or the horizontal line) and mixed-eye dominance (seeing various partial combinations of the two lines). Cogan found that transitions between the single-eye-dominant images or between the mixed-eye-dominant images (which we call trapping here) were less likely than other transitions (in which changes in eye dominance were not synchronized across the visual field).

Stimulus specificity of trapping implies that the strong component of trapping depended on pattern processing. What figural characteristics might then be critical for producing strong trapping? Note that trapping
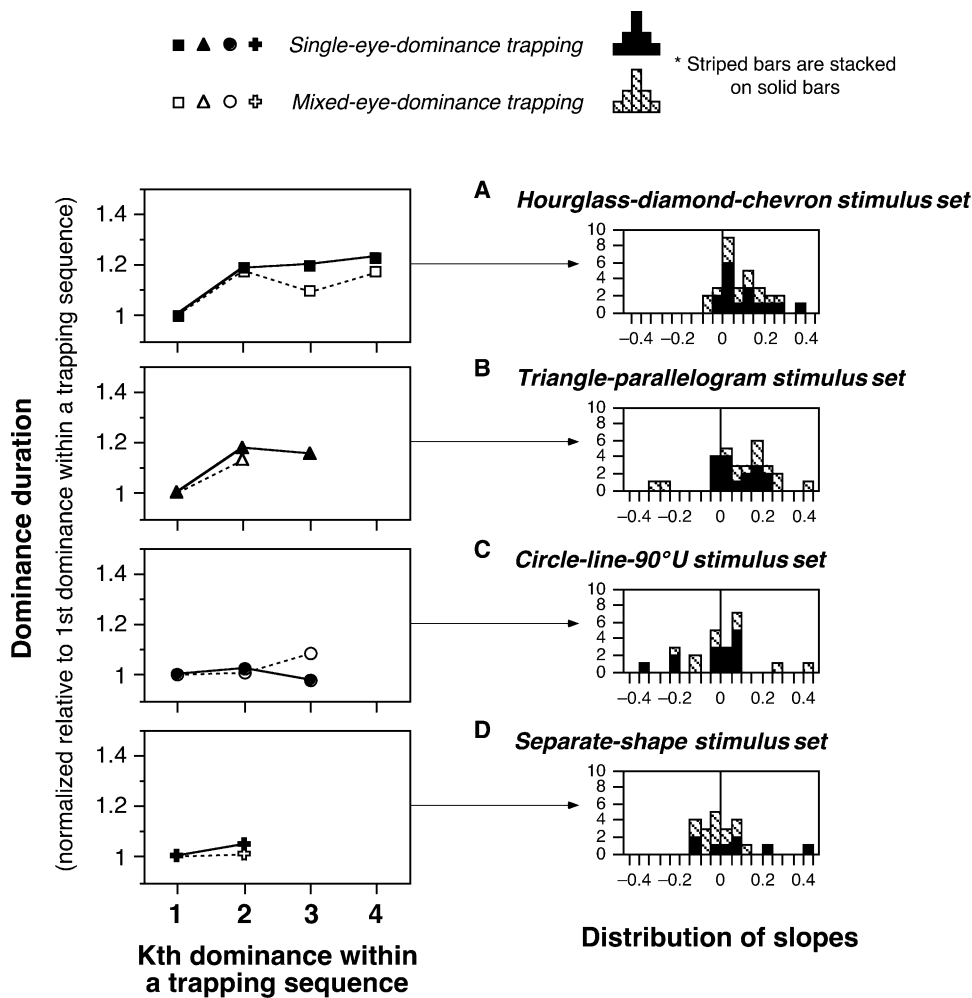
Figure 5. Changes in Dominance-Phase Duration during Trapping

In the left panels, the dominance-phase duration (normalized relative to 1st dominance) is plotted as a function of the kth dominance within a trapping sequence. To illustrate overall trends, the data were averaged for each stimulus set across observers and across all perceived images, but averaged separately for single-eye dominance trapping (filled symbols) and mixed-eye-dominance trapping (open symbols). The linear slope of the functions illustrated in the left panel was computed for each perceived image under each of the two types of eye dominance for each observer, and the distributions of these slopes are plotted in the right panels. Negative values would indicate adaptation (sequential reductions in dominance-phase durations) during trapping.

greater than 1/3 was flatly absent only for the separate-shape stimulus set (Figure 3D). Because each perceived image in this stimulus set consisted of two separate shapes whereas the perceived images in the rest of the stimulus sets were all unitized patterns, rivaling images being single unitized patterns might be critical for producing strong trapping. However, unitized images per se did not guarantee substantial trapping because trapping beyond 1/3 was also virtually absent between the left and the right 90° U patterns (Figure 3C, right bars); trapping also did not occur in the aforementioned study by Cogan (1972) though she used single (unitized) line segments. What other figural factors might distinguish between the pairs of images that produced strong trapping and the pairs of images that did not?

Returning to our initial hypothesis, multistable perception might tend to get trapped within a pair of *related* patterns. In the case of the circle-line-90° U stimulus set, the concentric-circle pattern and the horizontal-line pattern (that produced trapping beyond 1/3) might both

be processed together at some stage as *bilaterally symmetric* patterns. In contrast, the left and the right 90° U patterns (that did not produce trapping beyond 1/3) do not appear to have any salient global property in common. The effect of bilateral symmetry could also explain why trapping in the separate-shape stimulus (though minimal overall) was relatively higher for the images that had the same contrast polarity on both sides than for the images that had opposite contrast polarity on either side (a small effect but obtained from all observers; see Figure 3D). Uniform contrast polarity on both sides might be processed as bilateral symmetry due to grouping by color or contrast polarity. As discussed earlier, in the case of the hourglass-diamond-chevron and the triangle-parallelogram stimulus sets which produced the most substantial trapping, we have some psychophysical evidence that suggests that each pair of images that produced strong trapping are related in that they may be encoded as opponent shape features.

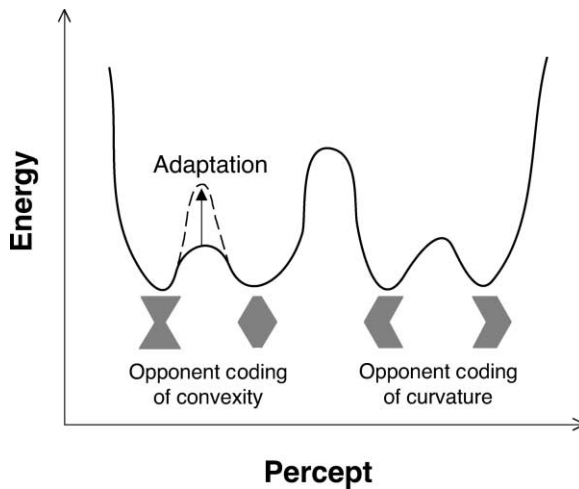Recently, Suzuki and colleagues and others demon-

Figure 6. A Schematic Potential-Energy Diagram to Account for Trapping and for Postselection Adaptation during Trapping

The diagram shows an example of multistability for the hourglass-diamond-chevron stimulus set. The four stable percepts correspond to the local minima (or attractors). The potential barriers are lower between percepts within the same opponent coding (e.g., between concave hourglass and convex diamond within the coding of convexity, and between left-pointing and right-pointing chevrons within the coding of curvature), and higher between percepts across different opponent codings (e.g., across the coding of convexity and the coding of curvature). When a percept is trapped within the coding of convexity, the potential barrier separating the convex and concave shape might rise (dashed curve), making the percept relatively more likely to break from the trapping and shift to one of the chevrons, while at the same time increasing the dominance durations of the convex and concave shapes (see text).

strated opponent shape aftereffects (using brief sequences of adaptation and test stimuli) that are tolerant for translation, scaling, and/or changes in surface features between adaptation and test, suggesting that global opponent coding exists for basic shape features such as convexity, overall curvature, taper, skew, and aspect ratio (e.g., Regan and Hamstra, 1992; Rivest et al., 1997, ARVO, abstract; Rivest et al., 1998, ARVO, abstract; Suzuki, and Cavanagh, 1998; Suzuki, 1999, ARVO, abstract; Suzuki, 2001, ARVO, abstract; Suzuki, 2002, VSS, abstract). Trapping might occur because perception tends to get "stuck" within a particular opponent coding. The trapping between the (concave) hourglass and the (convex) diamond might be due to getting stuck within the opponent coding of convexity; the trapping between the (left-pointing and right-pointing) chevrons might be due to getting stuck within the opponent coding of curvature; the trapping between the (top-tapered and bottom-tapered) triangles might be due to getting stuck within the opponent coding of taper; the trapping between the (right-skewed and left-skewed) parallelograms might be due to getting stuck within the opponent coding of skew.

This idea may be illustrated using a potential-energy diagram (or attractor; cf. Morita and Suemitsu, 2002). For example, consider the hourglass-diamond-chevron stimulus set (Figure 6). The four competing percepts, the hourglass, the diamond, the left chevron, and the right chevron correspond to the local minima (or attractors). The potential barrier is lower between per-

cepts within the same opponent coding (e.g., within the coding of convexity or within the coding of curvature), but higher across different opponent codings (e.g., across the coding of convexity and the coding of curvature). The percept changes as random (e.g., Poisson distributed) energy spontaneously exceeds a potential barrier. Trapping occurs because spontaneous transitions in percepts are more likely across a lower potential barrier (i.e., within the same opponent coding) than across a higher potential barrier (i.e., across different opponent codings).

An advantage of this model is that it could potentially account for the seemingly paradoxical adaptation effects that occurred during a trapping sequence; while the probability of continued trapping within an opponent pair tended to diminish (Figure 4), the dominance duration for each opponent shape tended to increase (Figure 5). These opposing trends on transition probability and dominance duration during trapping might be explained by postulating that the potential barrier between opponent shapes tends to rise during trapping. For example, while the percept is trapped within the opponent coding of convexity, the potential barrier between the convex and concave shapes might rise (dashed curves) to approach the height of the higher potential barrier over to the coding of curvature. Consequently, the spontaneous transitions between the convex and concave shapes would become no longer privileged (by the relatively lower potential barrier), and the percept should become more likely to break from the trapping and shift to one of the chevrons. As the percept then gets trapped within the opponent coding of curvature, the potential barrier within the coding of convexity might fall due to recovery from adaptation while the potential barrier between the opposite-curved shapes might rise, and so on. A rising potential barrier between opponent shapes could also make perception of each opponent shape increasingly more stable during trapping because it should take longer for random energy to spontaneously exceed a higher potential barrier. Thus, both the reduced probability of continued trapping and the lengthened dominance durations that occurred during a trapping sequence for opponent-shape multistable stimuli could be accommodated by postulating that a potential barrier between opponent shapes rises during trapping. Regardless of the eventual validity of this simple preliminary model, our results call for "adaptation" mechanisms beyond simple desensitization of relevant neural units, as desensitization should reduce dominance duration as well as transition probability.

We have so far suggested that trapping is likely due to influences from global pattern representations. What could be the mechanism of these high-level influences on multistable binocular rivalry? On the one hand, there have been numerous studies reporting influences of global-pattern and image-grouping processes on bistable binocular rivalry, suggesting that binocular rivalry involves influences from multiple cortical visual areas (e.g., Diaz-Caneja, 1928; Yu and Blake, 1992; Kovács et al., 1996; Logothetis et al., 1996; Logothetis, 1998; Bonneh and Sagi, 1999; Bonneh et al., 2001; see Blake and Logothetis, 2002 for a review). On the other hand, extensive research on binocular rivalry suggests that the primary mechanism of rivalry (at least for static stimuli) is ocular competition (i.e., competition between the non-

fusible signals coming from the two eyes; e.g., Blake and Fox, 1974; Lack, 1974; Blake et al., 1980, 1998; Blake, 1989; Lee and Blake, 1999); this competition appears to occur in the primary visual cortex (e.g., Polonsky et al., 2000; Tong and Engel, 2001). As demonstrated both by our present study and by other studies, ocular competition can occur separately in local regions (e.g., Levelt, 1965; Blake et al., 1992; Kovács et al., 1996; Wilson et al., 2001; Lee and Blake, 2002, VSS, abstract). We thus speculate that feedback from global pattern representations (in which trapping and adaptation presumably occur) might induce shape-based binocular rivalry by facilitating specific patterns of local dominance in V1. For example, feedback signals from an activated representation of convex shape might facilitate dominance of the diamond shape by enhancing the group of local edge detectors responding to the diamond contours such that those contours tend to gain dominance simultaneously in local rivalry.

The neural substrate of the relevant global pattern representations might be in the inferotemporal cortex (IT) because (1) IT cells are tuned to various global geometric shapes (e.g., Fujita et al., 1992; Ito et al., 1995; Logothetis and Sheinberg, 1996; Tanaka, 1996; Hikosaka, 1999), (2) about 90% of IT cells show substantial response modulations consistent with alternations of dominant percepts during binocular rivalry (e.g., Sheinberg and Logothetis, 1997; Logothetis, 1998), and (3) many IT cells adapt substantially within a second (e.g., Miller et al., 1993; Lueschow et al., 1994; Vogels, et al., 1995). Opponent coding of convexity, curvature, taper, and skew might exist in IT as suggested by the global opponent shape aftereffects mentioned above. Because cells involved in coding similar features tend to be clustered or organized into densely connected feature columns within IT (e.g., Hasselmo, et al., 1989; Fujita et al., 1992; Tanaka, 1996; Wang, et al., 1996, 2000; Renart et al., 2001; Tsunoda et al., 2001; see Barlow 1981 for a theoretical argument), the lower potential barrier within the coding of each opponent feature might be due to excitatory connections among the neighboring feature columns and the rising of the potential barrier might be due to increasing activity of inhibitory interactions among them (e.g., Wang et al., 2000; Renart et al., 2001) and/or to neural adaptation (see Figure 6).

Finally, Blake et al. (1990) reported short-term adaptation effects *for dominance-phase duration* in bistable binocular rivalry. They found that when one of the two competing images was forced to be in the dominance phase for a prolonged duration of time and then released from the forced dominance phase, its subsequent suppression was abnormally long and its subsequent dominance was abnormally short, but only in the immediately following cycle of dominance. They thus suggested that short-term adaptation might be involved in generating perceptual transitions in binocular rivalry. In contrast, the adaptation effects we obtained *for transition probabilities* during a trapping sequence in multistable rivalry occurred spontaneously without externally forced prolonged dominance, and they built up over several cycles of dominance. Furthermore, adaptation during trapping did not occur for dominance-phase duration; if anything, dominance durations increased over the course of trapping. It thus appears that the mechanism underlying the

forced short-term adaptation effects reported by Blake et al. (1990), potentially implicated in generating perceptual transitions, is distinct from the mechanism(s) underlying the slower spontaneous adaptation effect we obtained, potentially reflecting neural interactions at the level of opponent shape coding (Figure 6).

In conclusion, we have presented clear and systematic evidence of path dependence and postselection adaptation during multistable binocular rivalry, and explained these effects in terms of feedback from adaptable high-level pattern coding. Perception tended to get trapped within a pair of images that were potentially coded as related patterns at some level of processing (e.g., the processing of figural opponency and bilateral symmetry). Furthermore, when trapping occurred between two opponent shapes (as defined by shape aftereffects), the visual system tended to adapt to those shapes (i.e., transition probabilities to return to them were reduced) during the course of trapping. These results suggest that perceptual multistability provides a psychophysical tool for elucidating high-level pattern coding and its adaptation. Future research using a large sample of stimuli will be necessary to precisely define the image features that underlie trapping and to determine whether the mechanisms of trapping and adaptation are intimately related as is suggested in Figure 6.

Experimental Procedures

Observers
Five trained psychophysical observers C.K., E.T., Y.S., D.G., who were naïve to the experimental hypotheses, and S.S. (one of the authors) volunteered (or were paid) to participate. Observers C.K., E.T., and Y.S. participated in all experiments; D.G. participated only in the main experiment and S.S. participated only in the control experiments. All observers had normal or corrected-to-normal vision, and were tested individually in a normally lit room.

The Main Experiment
Apparatus
Stimuli were displayed on a 19" color monitor (75 Hz) and the experiment was controlled with a Macintosh PowerPC 8600 (300 MHz) computer using Macromedia director 6.5 (Macromedia, Inc.). A stereoscope consisting of four right-angle prisms and a central divider was used to present stimuli dichoptically.
Stimuli
The stimulus dimensions are shown in Figures 1A and 1C. The side contours of the shapes in the hourglass-diamond-chevron stimulus set were tilted 25° from vertical, and the side contours of the shapes in the triangle-parallelogram stimulus set were tilted 30° from vertical. All stimuli were presented against a white background (122 cd/m², CIE[.31,.34]). The shapes were dark green (62 cd/m², CIE[.34,.49]) and presented within a binocularly viewed high-contrast black frame (13 cd/m²) that was checkerboard textured to facilitate binocular fusion. A bullseye fixation marker (binocular and black) was presented at the center. The viewing distance was 115 cm.
Procedure
At the beginning of each trial, observers saw the textured frame with only the fixation marker inside. Upon confirming stable binocular fusion of the fixation marker and the frame, the experimenter presented one of the four dichoptic pairs of shapes (Figures 1A–1D); observers then viewed the stimulus continuously. While maintaining fixation at the fixation marker, observers named the perceived shape whenever a new shape became dominant, using "hourglass" for the hourglass, "diamond" for the diamond, "up" for the upright triangle, "down" for the inverted triangle, "left" for the left-pointing chevron or the left-skewed parallelogram, and "right" for the right-pointing chevron or the right-skewed parallelogram. When none of the four shapes was exclusively visible, observers named the apparently

dominant shape. When none of the shapes was apparently domi-
nant, observers called out "equal." The "equal" responses occurred
infrequently (less than 1.7%) and for only one observer (C.K.). The
experimenter terminated the display when a dominant phase ended
past 60 s. At least a 5 min break was given prior to the next trial.
The verbal responses were tape-recorded (and digitized), and the
time intervals between responses (i.e., the durations of the dominant
percepts) were obtained by examining the audiogram (using
SoundEdit 16, Macromedia Inc.).

In each experimental session, eight trials were tested, with the
four dichoptic pairs (Figures 1A–1D) counterbalanced for the two
eyes. Half of the observers were tested in the following order in
their first session: the inverted triangle to left eye and the upright
triangle to right eye, the right-skewed parallelogram to left eye and
the left-skewed parallelogram to right eye, the diamond to left eye
and the hourglass to right eye, the left-pointing chevron to left eye
and the right-pointing chevron to right eye, followed by the four
pairs being repeated with the left-eye shape and the right-eye shape
swapped. The other half of the observers were tested in the reverse
order. Each session took 1–1.5 hr. To obtain sufficient data, each
observer was tested in eight sessions (typically one session per
day). The forward and reversed orders of the eight stimulus pairs
were alternated across sessions.

The Control Experiments
Apparatus
The same as in the main experiment except that Vision Shell soft-
ware (Micro ML, Inc.) was used for controlling the experiments.
Stimuli
The stimulus dimensions are shown in Figures 1E and 1G. To facili-
tate binocular alignment for these stimuli, which did not produce
simple unitized shapes, the inner square frame was drawn in addition
to the textured frame used in the main experiment. The circle-line-
90° U stimulus set (Figures 1E and 1F) was used in the first control
experiment. To further facilitate binocular alignment, the middle ver-
tical line was added. The width and spacing of the lines forming the
patterns were both 0.074°. The white parts had the luminance of
102 cd/m^2 (CIE[.30,.34]) and the black parts had the luminance of
20 cd/m^2 (CIE[.36,.39]). The separate-shape stimulus set (Figures
1G and 1H) was used in the second control experiment. The contrast
polarity of the shapes was reversed across the two eyes to generate
clear rivalry for these shapes. The white shapes had the luminance
of 120 cd/m^2 (CIE[.30,.34]), the black shapes had the luminance of
20 cd/m^2 (CIE[.36,.39]), and the immediate background of the shapes
was mid-gray (50 cd/m^2, CIE[.32,.36]); the Michelson contrasts of
the white and the black shapes were thus about ± 0.4. Other aspects
of the stimuli were the same as in the main experiment.
Procedure
Generally the same as in the main experiment. During each 60 s
trial, the observer named the perceived shape whenever a new
shape became dominant. For the circle-line-90° U stimulus set, the
names used were "circles," "lines," "left" (for 90° U with curved
texture on the left), and "right" (for 90° U with curved texture on the
right). For the separate-shape stimulus set, observers named each
pair of dominant shapes from left to right, "plus-circle," "x-square,"
"plus-square," and "x-circle." Note that observers named the newly
dominant pair whenever both or one shape changed. These verbal
responses were tape-recorded as in the main experiment. One pro-
cedural change was that the coding of duration of each dominance
phase was made more efficient; it was unduly time consuming to
manually analyze audiograms. As observers named each dominant
shape, they also clicked the trigger switch (always the same switch)
on a hand-held joy stick to automatically record the beginning of
each dominance. A sample of the audiogram and trigger switch
responses were evaluated to verify that they produced comparable
results.

For the first control experiment (using the circle-line-90° U stimu-
lus set), four trials were tested in each session, with the two dichoptic
pairs (Figures 1E and 1F) counterbalanced for the two eyes. All
orders of the four pairs (excluding immediate repetitions of the same
pair) were tested in eight sessions. For the second control experi-
ment (using the separate-shape stimulus set), only the pair shown
in Figure 1G was initially tested; four trials were tested in each

session, counterbalancing for the contrast polarity assignment
(black versus white) and the two eyes. All orders of the four pairs
(excluding immediate repetitions of the same shape-eye assign-
ment) were tested in four sessions. The stimulus shown in Figure
1H was subsequently tested in the same way such that the stimulus
manipulation for the separate-shape stimulus set was comparable
to that for the rest of the stimulus sets (i.e., each pattern on the left
side being paired with each pattern on the right side). At least a 5
min break was inserted between trials and at least a 10 min break
was inserted between sessions.

Computation of the Probability that the Left and the Right
Sides of the Image Change Synchronously Assuming
that Binocular Rivalry Occurs Independently
on the Two Sides
If binocular rivalry occurs independently on either side, the chance
probability of synchronous changes on both sides (i.e., chance prob-
ability of trapping) should depend critically on the perceptual inte-
gration time, Δt, which we define as *the minimum time required for
a transition in the perceived image to occur and during which eye-
dominance transitions on the two sides are seen as being simultane-
ous*. A shorter Δt would predict a smaller probability of synchronous
changes. A conservative (i.e., a long) estimate of Δt for each stimulus
is given by the minimum observed dominance-phase duration. Each
dominance-phase duration (measured from the beginning of domi-
nance of the current image to the beginning of dominance of the
next image) includes the stable dominance of the current image
plus the transition time, Δt, to the next image. Thus, if we assume that
Δt is relatively constant for each stimulus, the minimum dominance-
phase duration obtained for a given stimulus (in which the stable
duration component is minimal) would provide an estimate of Δt
for the stimulus. Once Δt is obtained, the probability of an eye-
dominance transition that is expected to occur within Δt can be
computed for each side of the stimulus as:

$$p\,(\text{transition on left side within } \Delta t) =$$

$$\frac{\text{Total \# of dominance transitions on left side}}{\text{Total time of observation}} \times \Delta t$$

for the left side and

$$p\,(\text{transition on right side within } \Delta t) =$$

$$\frac{\text{Total \# of dominance transitions on right side}}{\text{Total time of observation}} \times \Delta t$$

for the right side (assuming that the transition probability is station-
ary on each side). The probability of an eye-dominance change
occurring synchronously on both sides (within Δt) is then given by:

$$p\,(\text{synchronous transition}) = p\,(\text{transition on left side within } \Delta t) \times$$

$$p\,(\text{transition on right side within } \Delta t) \equiv p\,(L) \times p\,(R).$$

The relative probability, p_r, of synchronous changes (as compared
with asynchronous changes) commensurate with the values ob-
tained from Equation 1 (and plotted in Figure 3) is then given by,

$$p_r\,(\text{synchronous transition}) =$$

$$\frac{p\,(L) \times p\,(R)}{p\,(L) \times p\,(R) + \{1 - p\,(L)\} \times p\,(R) + p\,(L) \times \{1 - p\,(R)\}}.$$

In Figure 3, these "chance probabilities of trapping" expected from
independent rivalry occurring on either side are indicated with
dashed lines for each stimulus set for each observer. As expected,
these probabilities are much lower than 1/3.

References

Attneave, F. (1971). Multistability in perception. Sci. Am. *225*, 62–71.

Barlow, H.B. (1981). Critical limiting factors in the design of the eye and visual cortex. Proc. R. Soc. Lond. B Biol. Sci. *212*, 1–34.

Blake, R. (1989). A neural theory of binocular rivalry. Psychol. Rev. *96*, 145–167.

Blake, R., and Fox, R. (1974). Binocular rivalry suppression: Insensitive to spatial frequency and orientation change. Vision Res. *14*, 687–692.

Blake, R., and Logothetis, N.K. (2002). Visual competition. Nat. Neurosci. *3*, 1–11.

Blake, R., Fox, R., and McIntyre, C. (1971). Stochastic properties of stabilized-image binocular rivalry alternations. J. Exp. Psychol. *88*, 327–332.

Blake, R., Westendorf, D.H., and Overton, R. (1980). What is suppressed during binocular rivalry? Perception *9*, 223–231.

Blake, R., Westendorf, D.H., and Fox, R. (1990). Temporal perturbations of binocular rivalry. Percept. Psychophys. *48*, 593–602.

Blake, R., O'Shea, R.P., and Mueller, T.J. (1992). Spatial zones of binocular rivalry in central and peripheral vision. Vis. Neurosci. *8*, 469–478.

Blake, R., Yu, K., Lokey, M., and Norman, H. (1998). Binocular rivalry and motion perception. J. Cogn. Neurosci. *10*, 46–60.

Bonneh, Y., and Sagi, D. (1999). Configuration saliency revealed in short duration binocular rivalry. Vision Res. *39*, 271–281.

Bonneh, Y., Sagi, D., and Karni, A. (2001). A transition between eye and object rivalry determined by stimulus coherence. Vision Res. *41*, 981–989.

Borsellino, A., De Marco, A., Allazetta, A., Rinesi, S., and Bartolini, B. (1972). Reversal time distribution in the perception of visual ambiguous stimuli. Kybernetik *10*, 139–144.

Cavanagh, P. (1992). Attention based motion perception. Science *257*, 1563–1565.

Cogan, R. (1972). Patterns of changes in binocular contour rivalry. Percept. Mot. Skills *35*, 569–570.

Cogan, R. (1973). Distributions of durations of perception in the binocular rivalry of contours. J. Gen. Psychol. *89*, 297–304.

Diaz-Caneja, E. (1928). Sur l'alternance binoculaire. Annual Oculist. 721–731, cited in Logothetis, N.K. (1998). Single units and conscious vision. Philos. Trans. R. Soc. Lond. B. Biol. Sci., B, *353*, 1801–1818.

Fox, R., and Herrmann, J. (1967). Stochastic properties of binocular alternations. Percept. Psychophys. *2*, 432–436.

Fujita, I., Tanaka, K., Ito, M., and Cheng, K. (1992). Columns for visual features of objects in monkey inferotemporal cortex. Nature *360*, 343–346.

Hasselmo, M.E., Rolls, E.T., and Baylis, G.C. (1989). The role of expression and identity in the face-selective responses of neurons in the temporal visual cortex of the monkey. Behav. Brain Res. *32*, 203–218.

Hikosaka, K. (1999). Tolerances of responses to visual patterns in neurons of the posterior inferotemporal cortex in the macaque against changing stimulus size and orientation, and deleting patterns. Behav. Brain Res. *100*, 67–76.

Ito, M., Tamura, H., Fujita, I., and Tanaka, K. (1995). Size and position invariance of neuronal responses in monkey inferotemporal cortex. J. Neurophysiol. *73*, 218–226.

Kovács, I., Papathomas, T.V., Yang, M., and Feher, A. (1996). When the brain changes its mind: Interocular grouping during binocular rivalry. Proc. Natl. Acad. Sci. USA *93*, 15508–15511.

Lack, L.C. (1974). Selective attention and the control of binocular rivalry. Percept. Psychophys. *15*, 193–200.

Lack, L.C. (1978). Selective Attention and the Control of Binocular Rivalry (The Hague: Mouton Publishers).

Lathrop, R.G. (1966). First-order response dependencies at a differential brightness threshold. J. Exp. Psychol. *72*, 120–124.

Lee, S.-H., and Blake, R. (1999). Rival ideas about binocular rivalry. Vision Res. *39*, 1447–1454.

Lehky, S.R. (1988). An astable multivibrator model of binocular rivalry. Perception *17*, 215–228.

Lehky, S.R. (1995). Binocular rivalry is not chaotic. Proc. R. Soc. Lond. B Biol. Sci. *259*, 71–76.

Levelt, W.J.M. (1965). On Binocular Rivalry (Soesterberg, The Netherlands: Institute for Perception RVO-TNO).

Logothetis, N.K. (1998). Single units and conscious vision. Philos. Trans. R. Soc. Lond. B. Biol. Sci. *353*, 1801–1818.

Logothetis, N.K., and Sheinberg, D.L. (1996). Visual object recognition. Annu. Rev. Neurosci. *19*, 577–621.

Logothetis, N.K., Leopold, D.A., and Sheinberg, D.L. (1996). What is rivalling during binocular rivalry? Nature *380*, 621–624.

Lueschow, A., Miller, E.K., and Desimone, R. (1994). Inferior temporal mechanisms for invariant object recognition. Cereb. Cortex *5*, 523–531.

Miller, E.K., Li, L., and Desimone, R. (1993). Activity of neurons in anterior inferior temporal cortex during a short-term memory task. J. Neurosci. *13*, 1460–1478.

Morita, M., and Suemitsu, A. (2002). Computational modeling of pair-association memory in inferior temporal cortex. Cogn. Brain Res. *13*, 169–178.

Peterson, M.A., and Gibson, B.S. (1991). Directing spatial attention within an object: Altering the functional equivalence of shape description. J. Exp. Psychol. Hum. Percept. Perform. *17*, 170–182.

Peterson, M.A., Harvey, E.M., and Weidenbacher, H.J. (1991). Shape recognition contributions to figure-ground reversal: Which route counts? J. Exp. Psychol. Hum. Percept. Perform. *17*, 1075–1089.

Polonsky, A., Blake, R., Braun, J., and Heeger, D.J. (2000). Neuronal activity in human primary visual cortex correlates with perception during binocular rivalry. Nat. Neurosci. *3*, 1153–1159.

Ramachandran, V.S., and Anstis, S.M. (1983). Perceptual organization in moving patterns. Nature *304*, 529–531.

Regan, D., and Hamstra, S.J. (1992). Shape discrimination and the judgment of perfect symmetry: dissociation of shape from size. Vision Res. *32*, 1845–1864.

Renart, A., Moreno, R., de la Rocha, J., Parga, N., and Rolls, E.T. (2001). A model of the IT-PF network in object working memory which includes balanced persistent activity and tuned inhibition. Neurocomputing *38–40*, 1525–1531.

Richards, W., Wilson, H.R., and Sommer, M.A. (1994). Chaos in percepts? Biol. Cybern. *70*, 345–349.

Sheinberg, D.L., and Logothetis, N.K. (1997). The role of temporal cortical areas in perceptual organization. Proc. Natl. Acad. Sci. USA *94*, 3408–3413.

Sugie, N. (1982). Neural models of brightness perception and retinal rivalry in binocular vision. Biol. Cybern. *43*, 13–21.

Suzuki, S. (2001). Attention-dependent brief adaptation to contour orientation: a high-level aftereffect for convexity? Vision Res. *41*, 3883–3902.

Suzuki, S., and Cavanagh, P. (1998). A shape-contrast effect for briefly presented stimuli. J. Exp. Psychol. Hum. Percept. Perform. *24*, 1315–1341.

Suzuki, S., and Peterson, M.A. (2000). Multiplicative effects of intention on the perception of bistable apparent motion. Psychol. Sci. *11*, 202–209.

Tanaka, K. (1996). Inferotemporal cortex and object vision. Annu. Rev. Neurosci. *19*, 109–139.

Taylor, M.M., and Aldridge, K.D. (1974). Stochastic processes in reversing figure perception. Percept. Psychophys. *16*, 9–27.

Tong, F., and Engel, S.A. (2001). Interocular rivalry revealed in the human cortical blind-spot representation. Nature *411*, 195–199.

Tsunoda, K., Yamane, Y., Nishizaki, M., and Tnifuji, M. (2001). Com-

plex objects are represented in macaque inferotemporal cortex by the combination of feature columns. Nat. Neurosci. *4*, 832–838.

Verstraten, F.A.J., Cavanagh, P., and Labianca, A.T. (2000). Limits of attentive tracking reveal temporal properties of attention. Vision Res. *40*, 3651–3664.

Vogels, R., Sáry, G., and Orban, G.A. (1995). How task-related are the responses of inferior temporal neurons? Vis. Neurosci. *12*, 207–214.

Wade, N.J. (1974). The effect of orientation in binocular contour rivalry of real images and afterimages. Percept. Psychophys. *15*, 227–232.

Wade, N.J. (1975). Binocular rivalry between single lines viewed as real images and afterimages. Percept. Psychophys. *17*, 571–577.

Wang, G., Tanaka, K., and Tanifuji, M. (1996). Optical imaging of functional organization in the monkey inferotemporal cortex. Science *272*, 1665–1668.

Wang, Y., Fujita, I., and Maruyama, Y. (2000). Neuronal mechanisms of selectivity for object features revealed by blocking inhibition in inferotemporal cortex. Nat. Neurosci. *3*, 807–813.

Wilson, H.R., Blake, R., and Lee, S.-H. (2001). Dynamics of travelling waves in visual perception. Nature *412*, 907–910.

Yu, K., and Blake, R. (1992). Do recognizable figures enjoy an advantage in binocular rivalry? J. Exp. Psychol. Hum. Percept. Perform. *18*, 1158–1173.